Journal of Materials Chemistry A

Accepted Manuscript

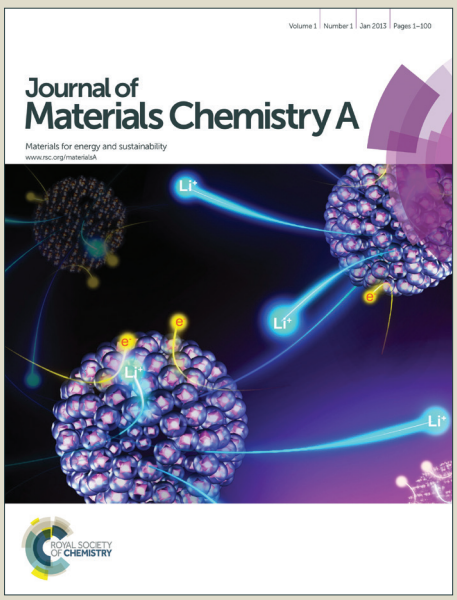

ROYAL SOCIETY OF CHEMISTRY

www.rsc.org/materialsA

Manipulating the horizontal morphology and vertical distribution of the active layer in BHJ-PSC with multi-function solid organic additive

Chun-Guey Wu[a,b,*]; Chien-Hung Chiang[b]; Hsieh-Cheng Han[b]

* [a] Professor: Chun Guey Wu,
Department of Chemistry, National Central University,
Jhong-Li, Taiwan 32001, ROC
Fax: 886-3-4227664
E-mail: t610002@cc.ncu.edu.tw

[b,] Research Center for New Generation Photovoltaics, National Central University, Jhong-Li, Taiwan 32001, ROC.

Abstract:

A new type of simple organic solid, 2,3-pyridinediol, was added in the active layer of Bulk Hetero-Junction Polymer Solar Cell (BHJ-PSC) to improve the processing and power conversion efficiency (PCE) of the devices. 2,3-pyridinediol additive with pyridyl and hydroxyl groups can interact with both P3HT and $PC_{61}BM$ (*via* π–π interaction or/and hydrogen-bonding) to reorganize the phase/domain and vertical distribution of the blended film. Therefore, even without thermal annealing, P3HT/$PC_{61}BM$/2,3-pyridinediol film forms the bicontinueous interpenetrated nano-domain networks with more P3HT close to PEDOT:PSS anode. 2,3-pyridinediol additive also can improve the efficiency of BHJ-PSC based on other n-type material such as ICBA (PCE of the device based on ICBA/P3HT increases from 3.35 to 5.93% after adding additive) and p-type material such as PTB7 (PCE of the device used PTB7/$PC_{71}BM$ active layer increases from 5.30 to 7.54% after adding additive). Moreover the thermal stability of PTB7/$PC_{71}BM$/2,3-pyridinediol blended film is better than PTB7/$PC_{71}BM$ blend with 1,8-diiodooctane. When the active films were heated at 100 ^{o}C for 30 min, the PCE of PSC based on PTB7/$PC_{71}BM$/ 1,8-diiodooctane decreases 20% (from 6.62% to 4.26%) whereas the PCE of PSC used PTB7/$PC_{71}BM$/ 2,3-pyridinediol blended film as an active layer decreases only *ca.* 3% (7.54% decreases to 7.30%). Small molecule solid additive in the active layer can mix well with the active components and will not be removed in the device fabrication processes. Therefore the morphology of the active film can be well-controlled and PCEs of the corresponding devices are more reproducible.

Keywords: Polymer solar cell, Additive, 2,3-pyrridinediol, P3HT, PCBM, ICBA, PTB7.

1. Introduction

High efficiency, low fabrication costs combined with solution processing and flexibility made organic photovoltaics (OPVs) a potential candidate for the next generation low-cost solar cells.[1-4] Inverted bulk hetero-junction polymer solar cell (BHJ-PSC) incorporating low-band gap conjugated polymer (such as PTB7[4] or PBTl3T[5]) and fullerene derivatives have achieved the power conversion efficiency (PCE) approximated to 9%.[5-9] Furthermore, tandem cell based on the oligomers with PCE value up to 12% has also been certified.[10] In a BHJ-PSC, the morphology of the polymer blend (active layer) has a crucial influence on the photo physics of the active film and performance of the corresponding device.[11,13] However, controlling the morphology of the active film to obtain the best performance of the device is extremely difficult since the optimal morphology of the active layer is not thermodynamically stable. As a result, the nano scale morphology of the active layer (film) is greatly affected by the film processing conditions and the best morphology can be obtained only by kinetically controlling the non-equilibrium state. Therefore, optimizing the active layer processing conditions using methods such as thermal[14-16] or solvent[17-19] annealing or additives[20-23] is necessary to achieve the high efficiency of the device. Among these methods, adding additive in the active layer is the simplest and most effective way.

The work of using additive starts with Bazan and coworkers[24] who found that adding n-octylthiol in P3HT/$PC_{61}BM$ blend dramatically enhanced the structural order of P3HT domain. As a result, the hole mobility increased by two orders of magnitude. In the following year, Heeger and coworkers[21] used 1,8-octanedithiol as an additive in PCPDTBT/$PC_{71}BM$ system and found that PCE of the device increases

from 2.8 to 5.5% with additive. They believed that the increase in the structural order of PCPDTBT by adding 1,8-octanedithiol could be the reason for the increase in PCE. The same group later found that 1,8-diiodooctane (DIO)[25] can also be an effective additive to enhance the efficiency of BHJ-PSC. As the additive generally is a higher boiling point substance compared to the host solvent (such as 1,2-dichlorobenzene or chlorobenzene) and a good solvent for PCBM, therefore they believed that during the film drying process, PCBM stays longer in solution than the polymer. This may allow PCBM to reorganize, resulting in a better nanophase segregated structures with appropriate domain size.[26] Furthermore, Wei *et al.*[27] found that 1, 6-diiodohexane (DIH) additive induced not only higher polymer crystallinity (2.4 and 3.6 times in the out-of-plane and in-plane directions, respectively) but also decreased the average size of the aggregated $PC_{71}BM$ clusters to 30 nm (from 150 nm for the film without additive). Both Cheng[28] and Heeger[29] reported that 1-chloronaphthalene (CN) can also be a good processing additive; the PCE can be improved as a result of the increasing in *J*sc values. Now it is widely accepted that the function of the high boiling point liquid additive is to reduce the aggregation of n-type fullerene and enhance the crystallinity of the self-organized p-type polymer by its selective solubility towards one component. Furthermore, ferroelectric oxide,[30] Au nanoparticle,[31] discotic liquid crystal,[32] 4-bromoanisole,[33] C60-end capped P3HT,[34] diblock copolymers[35-37] and some others[38-39] all have been reported to be a processing additive to improve the performance of the BHJ-PSC, nevertheless, the detailed mechanism was not clearly addressed.

On the other hand, low-band gap conjugated polymer, such as PTB7[4] has many excellent properties, including broad absorption in the solar spectrum to ensure effective harvesting of the solar photons, high charge mobility for carriers transport, energy levels match those of the fullerenes to provide a large open-circuit voltage, and

enough offset for charge separation. PSC based on PTB7/$PC_{71}BM$ using DIO as an additive achieves the PCE of 7.40% (without DIO the PCE (3.92%) is very poor).[6] However, PTB7/$PC_{71}BM$ blend film is very thermally sensitive even with DIO additive. For example our experiments show that PCE of the BHJ-PSC based on PTB7:$PC_{71}BM$ with DIO additive decreases significantly (20%) when the active film was heated at 100 ^{o}C for 30 minutes. Therefore searching for new additive with new functionality to increase the thermal stability of the active film is also very important for the practical application of low band-gap polymer in BHJ-PSC.

In this article a new additive, 2,3-pyridinediol, for improving the photovoltaic performance and processing of BHJ-PSCs was reported. We first study the effect of 2,3-pyridinediol on the physical properties of P3HT/$PC_{61}BM$ blend and PCE of the corresponding device to investigate the functions of this new additive. Then we proved that 2,3-pyridinediol is an all-purpose additive, it can significantly improve the PCE of BHJ-PSC based on P3HT/ICBA and PTB7/$PC_{71}BM$ active films. Finally, we demonstrated that the thermal stability of PTB7/$PC_{71}BM$ blended film also increases in the presence of 2,3-pyridinediol additive.

2. Experimental

2.1. Chemicals and physicochemical studies

RR-P3HT (region-regularity > 95 %, from Rieke Metal Inc., America), PBT7 (1-Material Chemscitech Inc., Canada), and Fullerene derivatives ($PC_{61}BM$, $PC_{71}BM$ and ICBA, Solenne B. V., Netherlands) were purchased from the commercial resources and used without further purification. Uv/Vis absorption and PL spectra were recorded with a Hitachi U-4100 and F-7000 spectrometers, respectively. AFM images were obtained using a Digital Instruments Multimode Scanning Probe

Microscope (E-sweep, SEIKO Inc., Japan). The thickness of the active film was measured with a depth-profile meter (Veeco Dektak 150, USA). Five lines on the film of 1 cmx1 cm) were made by carefully scratching with a plastic tip and the average height between the hills and valleys is used to represent the film thickness. X-ray photoelectron spectra/ Electron Spectroscopy for Chemical Analysis were taken with a Perkin-Elmer PHI-590AM XPS/ESCA spectrometer system with a Cylindrical Mirror Electron (CMA) energy analyser. The X-ray sources were Al Kα at 600 W and Mg Kα at 400 W. XPS were taken at pass energy of 160 eV and 10 eV for survey scans and high-resolution scans, respectively. Data analysis was done with the OriginPro 8 software package. Surface energy of the blended films was measured with a contact angle measuring system (Sigma Force tensiometers) using Pendant Drop Method. H_2O and CH_2I_2 were used as probe liquids, the surface energy was calculated from the contact angle of the liquids on film surface using WORK (Owens, Wendt, Rabel and Kaelble) method. To determine the hole-only mobility, the devices of ITO/PEDOT:PSS (30 nm)/P3HT-PC_{61}BM (100 nm with and without additive)/Au (100 nm) were fabricated. The hole mobility of the active layer was determined using the space charge limiting current (SCLC) method.[40]

2.2. OPV device fabrication and photovoltaic performance measurements

P3HT and PC_{61}BM with 1:1 weight ratio are dissolved in 1 mL 1,2-dichlorobenzene (conc. for each component is 20 mg/mL) and then various amount of 2,3-pyridinediol was added, the mixture was stirred overnight. BHJ-PSC device was fabricated followed the literature report[39] except the preparation of the active layer. 30 nm layer of poly(3,4-ethylene-dioxythiophene): poly(styrenesulfonate) (PEDOT:PSS, from H.C. Stark Baytron P, PH 1000) was used as a hole transport layer, 20 nm calcium and 100-nm aluminum (or silver) were deposited on the blended film by thermal evaporation to be a cathode. The thickness of the active layer was

controlled by the spin rate. The active area of the device is 0.2 cm x 0.5 cm. P3HT/ICBA and PBT7/$PC_{71}BM$ systems were prepared with the similar process. The *J-V* curves of all devices are measured using a Keithley 4200 source-measuring unit. A calibrated solar simulator (Oriel) with 100 mW/cm^2 power density was used as the light source. The external quantum efficiency (EQE) was measured in air and a chopper and lock-in amplifier were used for the phase sensitive detection with QE-R3011 (Enlitech Inc., Taiwan).

3. Results and discussion

3.1 The effect of 2,3-pyridinediol additive on the PCE of BHJ-PSCs based on P3HT/PCBM blended films.

The current density-voltage (*J-V*) curves of P3HT/$PC_{61}BM$ based devices with or without 2,3-pyridinediol additive and with or without thermal annealing are displayed in Figure 1 and the photovoltaic data are listed in Table 1. Device based on the active layer without additive and thermal annealing (pristine film) presents poor photovoltaic characteristic (PCE: 1.53%) due to the fragmental phases were formed in the blended film during high rate (1600 rpm) spin[41] which significantly reduces the time available for P3HT to aggregate. Therefore higher efficiency (3.55%) is observed only when the active layer undergoes thermal annealing to reorganize both P3HT and $PC_{61}BM$ components. On the other hand, when 2,3-pyridinediol (20 mg 2,3-pyridinediol in 1 mL dichlorobenzene) is added in P3HT/$PC_{61}BM$ solution, without thermal annealing of the active film, the short-circuit current density (*J*sc) increases more than 2 times compared to that for the pristine device and the PCE value also significantly increases from 1.53% to 4.44%. Thermal annealing the active film with additive slightly increases the *V*oc and FF, however, *J*sc decreases (~ 10%) more significantly,

resulting in decreasing the PCE from 4.44% to 4.07%, see Table 1. Changing the amount of the additive in the active film does not increase the PCE of the device further. Optimizing the devices is also performed by changing the thickness of the active film (*via* changing the spin-coating rate) and the results show that the optimal thickness of the active film is *ca.* 350 nm (including 30 nm of PEDOT:PSS film, see Table 2). Data displayed in Table 1 and Table 2 show clearly that 2,3-pyridinediol can simplify the fabrication process (no thermal annealing needed) and improve the PCE (mainly in *J*sc and FF) of the devices. Simple fabrication process to achieve high device efficiency is a very important progress for the practical application of the low-cost BHJ-PSCs. Furthermore, in general the maximum efficiency of OPV based on P3HT/PCBM system occurs at the active film thickness less than 200 nm. Nevertheless, we found that the optimal thickness of P3HT/PCBM/additive film is higher than 300 nm. This unique phenomenon suggests that 2,3-pyridinediol additive has a special impact on the organization of P3HT and PCBM, therefore thicker active film still has high efficiency. In the following several paragraphs we will explore how 2,3-pyridinediol affects the organization of P3HT and PCBM, and the physicochemical and photovoltaic properties of the resulting blended film.

3.2 The effect of 2,3-pyridinediol additive on the physicochemical properties of P3HT/PCBM blended film and EQE of the corresponding BHJ-PSC devices.

UV-Visible absorption spectra of P3HT/$PC_{61}BM$ containing 2.0 wt% 2,3-pyridinediol with and without thermal annealing are illustrated in Figure 2 (a). The absorption spectra of the pristine films are also displayed in Figure 2 (a) as references. All films are spin-coated from the respective solutions under identical conditions with the spin speed of 1600 rpm. The absorption over the visible range belongs to P3HT and the intensity of the characteristic vibronic peaks at 510, 550 nm

and 603 nm is an indication for the crystallinity of P3HT domains.[42,43] Qualitatively, the ratio of the absorbance for 603 nm (which has been assigned to a highly inter-chain delocalized excitation[44]) and 550 nm peaks can be correlated to the local order of P3HT: the stronger 603 nm peak, the better crystalinity of P3HT.[45] The λ_{max} of the blended films with additive is slightly red-shifted by 4 nm compared to that of the pristine films (for both with and without thermal annealing) and the higher intensity of 603 nm peak, indicating that the additive can increase the order of P3HT domains. Furthermore, the peak intensity at 603 nm only decreases very slightly when the blended film with 2,3-pyridinediol additive is thermally annealed, implying that the order of P3HT domains in the film with additive already forms at room temperature and the ordered domains are thermally stable.

To probe the charge transfer between P3HT donor and fullerene acceptor in the active films, photoluminescence (PL) spectra (also illustrated in Figure 2 (a)) were taken by exciting the blended film with 580 nm light. The PL signal from P3HT was quenched significantly by adding 2,3-pyridinediol into the blended film, indicating more efficient photo induced charge transfer occurred between P3HT and PCBM (or P3HT and additive).[46-49] Additive seems to either assist the formation of the ordered P3HT phase to facilitate the exciton/charge migration[48] or to increase the interfacial area between P3HT and $PC_{61}BM$ (or between P3HT and 2,3-pyridinediol) for exciton dissociation by reducing the aggregation of P3HT. Moreover, the PL intensity of the active film with additive increases upon heating, indicating the aggregation of P3HT domains with the crystallinity (not the size of the ordered domains) of the domains intact as observed in the absorption spectra. Heating the blended film with additive also induced the growth of $PC_{61}BM$ domains as seen with the optical microscope (see Figure S1 of the Electron Supporting Information (ESI)). Oversized P3HT and $PC_{61}BM$ domains reduced the interfacial area between P3HT and $PC_{61}BM$ in the

active layer may be the reason for the decreasing in *J*sc of the device. However, large P3HT and PCBM domains may also facilitate the exciton/carrier transport (the charge recombination decreases) therefore *FF* and *Voc* slightly increase upon heating the active film. Thermal annealing may also induce better contact between P3HT (or $PC_{61}BM$) and electrode to increase *FF* value.

In a BHJ-PSC, after the excitons dissociate at the donor/acceptor interface, efficient carrier transport/collection is required for high *J*sc. EQE spectra (Figure 2 (b)) of the devices are taken to examine the changes in the carrier transport of the active films after adding 2,3-pyridinediol. The patterns of all EQE curves are essentially corresponding to the absorption spectra of the blended films in the range of 450–650 nm which is the absorption of P3HT but the values are significantly different for each device. Device based on the non-thermal active film with additive achieves the highest EQE values at the whole measured wavelength. Without thermal annealing, the absorption intensity of the active film with additive is only slightly stronger than that of the pristine film (see Figure 2(a)). Nevertheless the EQE values for the device based on the active film with additive are much higher, suggesting better exciton/carrier transporting pathways are formed in P3HT/$PC_{61}BM$ film with 2,3-pyridinediol additive. Furthermore, upon thermal annealing (150 ^{o}C, 30 min) the active film with additive, the EQE of the corresponding device decreases only slightly in the whole visible region (400 ~ 700 nm). The absorption, luminescence and EQE data consist with what has proposed in the previous paragraph that thermal annealing the active film induces the aggregation of P3HT and $PC_{61}BM$ to form bigger domains without changing the crystallinity (not crystal size) of P3HT domains. Thermal induced aggregation of P3HT is a benefit for the pristine film however it is not necessary for the film with additive which forms a bicontinuous interpenetrated network with suitable size for the exciton migration/dissociation and charge transport

at room temperature.

The hole-only mobility of BHJ-PSC based on P3HT/$PC_{61}BM$ active film with and without additive are measured using the space charge limited current (SCLC) method[35,40,50] and the results are also listed in Table 1. Without thermal annealing of the active layer, the mobility of the device based on the active film with additive is one order magnitude higher than that for the devices without additive. When the active film with additive was thermally annealed at 150 ^{o}C for 30 min, the mobility decreased probably due to the formation of some isolated P3HT or $PC_{61}BM$ domains. On the other hand, upon thermal annealing, the mobility for the devices based on the pristine film and film with additive is similar however *Jsc, FF* and PCE for the device based on the active film with additive are all higher. Therefore the hole mobility of the active film is not the major reason for the significantly improving in *Jsc* of the device based on active film with additive.

As discussed in the previous paragraphs and the literature reports[51,52] that morphology of the active layer is a very important factor for determining the photovoltaic performance of BHJ-PSCs. There are numerous investigations focus on exploring the morphology of P3HT/PCBM blend with assorted film processing conditions, additives and/or subsequent treatments using various physicochemical methods.[53-56] Here we used tapping mode AFM to collect simultaneously the topographic and phase images of the active films and displayed in Figure 3. The surface roughness obtained from the topographic images was 2.49, 2.83, 2.94, and 3.45 nm for the pristine film without thermal annealing, pristine film with thermal treatment, film with additive but without thermal annealing, and film with additive and thermal treatment, respectively. The surface roughness of the blend film increases upon heating and comparing to the pristine film, the surface roughness of the blend film with additive is higher. Higher surface roughness probably comes from the better

defined P3HT and $PC_{61}BM$ domains as supported by the phase images displayed on the right-hand side of Figure 3. The phase image of the pristine film without thermal annealing (Figure 3 (a)) reveals big, isolated $PC_{61}BM$ (dark) and P3HT (bright) domains. After thermal annealing, the interpenetrated morphology is formed (Figure 3 (b)) however the domain size of each phase is small (< 15 nm). Neither isolated domains nor small domain size is the optimal morphology for facilitating the exciton dissociation and charge transport simultaneously. On the other hand, in the presence of an additive, even without thermal annealing, a beautiful bicontinuous/ interpenetrated fiber-like network is formed (Figure 3 (c)). The bicontinuous nanoscale domains of P3HT and $PC_{61}BM$ phases are known[53-57] to be a proper morphology for the charge separation and transport. Furthermore, the diameter of each domain estimated from the cross section of the blend film with additive (the detail see Figure S2, ESI) is *ca.* 30 nm which is the optimal size for the exciton diffusion.[58] Heating the blended film (with additive) results in increasing the size of both P3HT and $PC_{61}BM$ domains but the interconnected fiber-like network preserves (see Figure 3 (d)). Thermal annealing the active film with additive leads to little oversized domains for the exciton diffusion/charge separation therefore *J*sc of the corresponding device decreases. Nevertheless, heating the active layer can improve the *V*oc and *FF*, probably also due to better wetting by the metal electrode or a structural change at the PEDOT:PSS/active layer interface.[59] As a result, the PCE of the device only slightly decreases after thermal annealing the active film with additive.

Interestingly, the phase images displayed in the right hand side of Figure 3 also reveal that the surface compositions for P3HT/$PC_{61}BM$ film with 2,3-pyridinediol are not the same as those for the pristine film. It seems that the surface of the pristine film is rich in P3HT (the lighter part), nevertheless, blended film with additive has more

$PC_{61}BM$ (the darker part) molecules on the surface for both thermal and non-thermal treated films. The vertical composition profile of the active film is also an important parameter for the photovoltaic performance of a BHJ-PSC. However, most studies are often limited to the film morphology. One of few examples focuses on studying the composition of the active film in vertical direction was carried out by Campoy-Quiles *et al*.[54] They used ellipsometry to study the vertical composition profiles of P3HT/$PC_{61}BM$ films under variable fabrication conditions (such as thermal annealing and post solvent treatment) and found that the pristine film spin coated on the fused silica (or PEDOT:PSS coated quartz) comprises a composition that varies from $PC_{61}BM$ rich close to the substrate to P3HT rich near the free (air) surface. After thermal treatment, some $PC_{61}BM$ molecules in the film move toward the film/air interface therefore the vertical composition profile changed. Here we used the depth profile ESCA analysis to probe the vertical composition profiles of the non-thermal treated P3HT/$PC_{61}BM$ films (with and without additive) deposited on PEDOT:PSS coated ITO and the results are displayed in the middle of Figure 4. In the pristine film (without additive), P3HT (represented by S atom) is rich in the film surface/air interface and then decreases gradually toward PEDOT:PSS coated anode and $PC_{61}BM$ (represented by O atom) increases accordingly, probably due to the strong interaction between the hydrophilic PEDOT:PSS and hydrophilic $PC_{61}BM$. This type of composition distribution is not good for the hole to transfer from P3HT to PEDOT:PSS coated anode. On the other hand, for the blended film with additive (surprisingly the content of additive (represented by N atom) is very homogeneous on the whole film therefore the atomic ratio of O can be used to represent the content of $PC_{61}BM$), the amount of P3HT increases toward the anode and $PC_{61}BM$ decreases accordingly, reverses the vertical distribution (see the middle of Figure 4). It seems that the additive has interacted with both P3HT and $PC_{61}BM$ to change their

hydrophobicity, therefore, more P3HT moves to PEDOT:PSS (anode) side (or more $PC_{61}BM$ diffuses to the film surface/air) to form a better vertical composition profile for the charge to transport: hole to anode *via* P3HT, electron to cathode *via* $PC_{61}BM$. The increasing in *J*sc for the device based on the film with additive may be also due to the redistribution of P3HT and $PC_{61}BM$ in the vertical direction of the blended film as demonstrated on the two sides of Figure 4.

3.3 **The functions of 2,3-pyridinediol additive**

The function of solid 2,3-pyridinediol additive will be different from the liquid additives reported previously.[20,23-29] Most (> 90%) of the liquid additive will be removed[19] after the active film was dried upon standing/heating whereas 2,3-pyridinediol remains in the active film even after thermal annealing. The reversed distribution of P3HT (or $PC_{61}BM$) in the film vertical direction and the homogeneous distribution of 2,3-pyridinediol in the blend film suggest that 2,3-pyridinediol interacts with both P3HT and $PC_{61}BM$. The interaction between 2,3-pyridinediol and P3HT (or $PC_{61}BM$) was supported by the following 3 evidences. The first: 2,3-pyridinediol is only very slightly soluble in $CHCl_3$, nevertheless, 2,3-pyridinediol/P3HT (1:1 weight ratio) and 2,3-pyridinediol/$PC_{61}BM$ (1:1 weight ratio) are all soluble in $CHCl_3$ (see Figure S3 of ESI); The second: ^{1}H-NMR (Figure 5, the full spectrum can be found in Figure S4, ESI)) peak for the H on O of 2,3-pyridinediol shifts up-field, becomes very sharp, and the integral area also increases (this is not a general phenomenon observed in ^{1}H-NMR for the hydrogen-bonded H) when $PC_{61}BM$ was added. NMR data suggest that in pure 2,3-pyridinediol there is a intramolecular (or intermolecular) hydrogen bonding between 2,3-pyridinediol, therefore the NMR signal is relatively broad. When PCBM was added, the carbonyl group from PCBM disrupts this intra-molecular

hydrogen-bonding of 2,3-pyridinediol by bi-dentate hydrogen-bonding (two hydroxyl groups from 2,3-pyridinediol interact with the carbonyl group together). Bi-dentate hydrogen-bonding potentially to be a stronger interaction than the intra-molecular hydrogen-bonding, therefore the proton signal upshifted and become sharp. Similar phenomenon was also observed in HOC-P3HT-COH and $PC_{61}BM$ reported by Chen *et al.*[60]; The third: the surface energy of P3HT and $PC_{61}BM$ films is 23.1 and 33.2 mN/m^2, respectively. On the other hand, the surface energy of 2,3-pyridinediol/P3HT (1:1 weight ratio) and 2,3-pyridinediol/$PC_{61}BM$ (1:1 weight ratio) is 63.8 and 50.9 mN/m^2, respectively (2,3-pyridinediol is very hydrophilic, therefore the contact angle of water on 2,3-pyridinediol film cannot be measured). These data suggest that 2,3-pyridinediol may interact with both P3HT and $PC_{61}BM$ in the blended film. The significant high surface energy of P3HT/2,3-pyridinediol blend may be one of the reasons that more P3HT moves to PEDOT:PSS side when P3HT/$PC_{61}BM$/ 2,3-pyridinediol was spin-coated on the top of PEDOT:PSS coated ITO. Considering the structure of all materials involved, it is reasonable to assume that the interaction between P3HT and additive is a π–π interaction and that between $PC_{61}BM$ and 2,3-pyridinediol is the hydrogen bonding, as shown in Figure 6. Certainly π–π interaction between $PC_{61}BM$ and 2,3-pyridinediol cannot be totally ruled out.

3.4 **2,3-pyridinediol was proved to be a general additive in varied active components to improve the photovoltaic performance of BHJ-PSC in various aspects**

The effects of this new solid additive imply that the bicontinuous interpenetrated morphology of the active film can be formed automatically at room temperature by adding additive. Moreover, the 3D organization/ distribution of the blended film can be manipulated by carefully selecting the functionality of the additive to change the

physical properties of the both components in the active film. To demonstrate the generality of using 2,3-pyridinediol as an additive in BHJ-PSC, ICBA acceptor[61] (instead of $PC_{61}BM$) or PTB7 donor[6] (instead of P3HT) is used as one of the active components. The photovoltaic parameters of the devices based on P3HT/ICBA and PTB7/$PC_{71}BM$ active films (with and without 2,3-pyridinediol additive) are listed in Table 3. Data in Table 3 demonstrate that 2,3-pyridinediol is also an effective additive to improve both *Jsc* and *FF* of the device using high LUMO energy acceptor or low band-gap polymer donor as one of the active components. Therefore, we believed that 2,3-pyridinediol is an all-purpose additive which can be employed in BHJ-PSC with various active components. Interestingly ICBA does not have the functional group to form hydrogen bonding with 2,3-pyridinediol however the additive also increase the photovoltaic performance of the device based on P3HT/ICBA. This result implies that π–π interaction may also occur between the additive and ICBA or π–π interaction between 2,3-pyridinediol and P3HT could be the major driving force for the formation of the optimal 3D organization in P3HT/ICBA film to improve the efficiency (mainly in *Jsc*) of the corresponding device.

Furthermore, as mentioned before that PTB7/$PC_{71}BM$ blended film is thermally sensitive even with DIO additive. We found that 2,3-pyridinediol additive also improve the thermal stability of PTB7/$PC_{71}BM$ film. For example: the PCE of BHJ-PSC based on PTB7/$PC_{71}BM$ with DIO additive without thermal annealing is 6.62%. However, when the active film was heated at 100 ^{o}C for 30 min, the PCE of the corresponding device dropped to 4.26%, due to the significantly decrease in the current density (see Table S1 of ESI). On the other hand, without thermal annealing the PCE of the device used PTB7/$PC_{71}BM$ with 2,3-pyridinediol as an active film is 7.54%. When PTB7/$PC_{71}BM$/2,3-pyridinediol film was heated at 100 ^{o}C for 30 min, PCE of the corresponding device slightly decreases to 7.30% (only 3% decrease,

detail also see Table S1 of ESI). 2,3-pyridinediol is a high boiling point (T_m = 245 ^oC; T_b = 387 ^oC) solid, it will not evaporate (the mobility is also low) during the heating or device fabrication process, therefore the thermal stability of the active layer can be improved with additive. 2,3-pyridinediol is also a simple organic molecule with multiple functionality (aromatic ring and OH group), therefore the effect of additive on the physical properties of the active film can be well-controlled and the photovoltaic performance of the corresponding BHJ-PSC is reproducible It is the merit of using solid 2,3-pyridinediol instead of high boiling point liquid as an additive in BHJ-PSC devices.

4. Conclusions

In summary we report a new solid organic additive, 2,3-pyridinediol, to increase the PCE of BHJ-PSC when thermal annealing of the active film is not needed. The morphology of the donor/acceptor network is critical to optimize the performance of the device. Nevertheless the vertical distribution of n-type and p-type materials in the active film is also a determining factor for achieving high PCE. We found that 2,3-pyridinediol not only induces the formation of the bicontinuous interpenetrate network with proper domain size but also regulated the vertical distribution of P3HT and $PC_{61}BM$ in the active film. The function of solid 2,3-pyridinediol additive is different from other reported liquid additives. Liquid additive influences the domain size of n-type fullerene and the crystallinity of p-type polymers by selective solubility towards fullerene and prolonging the solvent annealing time. On the other hand, 2,3-pyridinediol interacts with both active components (maybe to form a special supra-molecular architecture which still need more sophisticated studies to prove it) to change the polarity. Therefore optimal morphology was formed at room temperature

and P3HT distributes more close to PEDOT:PSS coated anode and the surface (air/film interface) has more $PC_{61}BM$, facilitate the charge transport. The effect of 2,3-pyridinediol additive is not specified it also can be applied to other n-type material such as ICBA and p-type low band-gap polymer such as PTB7 to improve the efficiency of the devices. It is also noteworthy that the thermal stability of the active layer is very important property for the long-term stability and therefore the practice applications of organic solar cells. Active film with 2,3-pyridinediol additive shows good thermal stability, owing to the additive has high boiling point (387 ^{o}C) (may also have the strong interaction with the active components). Moreover, if the 3D organizations/distributions of the active film in BHJ-PSC can be manipulated by the interaction between additive and active components, it is reasonable to assume that the thermodynamically unstable film morphology can be controlled by adding designed additive. Certainly much more studies are needed to find the right way. However, we believe that this result provides a new tract to simplify the fabrication process of BHJ-PSC, improve the thermal stability of the active layer and increase the PCE of the device by the additive with designed functionality.

Acknowledgement:

Financial support from the National Science Council (NSC), Taiwan, ROC was great acknowledged. The devices fabrication was carried out in Advanced Laboratory of Accommodation and Research for Organic Photovoltaics, NSC, Taiwan, ROC.

Supporting Information Available:

Some more detailed experimental data are collected in the supporting information. This material is available online with the article.

References

1 G.Yu, J. Gao, J. C. Hummelen, F. Wudl and A. J. Heeger, *Science,* 1995, **270**, 1789-1791.

2 C. Li, M. Liu, N. G. Pschirer, M. Baumgarten and K. Müllen, *Chem. Rev.,* 2010, **110**, 6817-6855.

3 M. A. Green, K. Emery, Y. Hishikawa and W. Warta, *Prog. Photovolt: Res. Appl.,* 2011, **19,** 84-92.

4. S. B. Daling and F. You, *RSC Adv.* 2013, **3**, 17633-17648.

5 Y. Liang, Z. Xu, J. Xia, S.-T. Tsai, Y. Wu, G. Li, C. Ray and L. Yu, *Adv. Mater.,* 2010, **22**, E135–E138.

6 X. Guo, N. Zhou, S. J. Lou, J. Smith, D. B. Tice, J. W. Hennek, R. P. Ortiz, J. T. L.; Li, S. Navarrete, J. Strzalka, L. X. Chen, R. P. H. Chang, A. Facchetti and T. J. Marks, *Nature Photonics,* 2013,**7**, 825-833

7 Z. He, C. Zhong, S. Su, M. Xu, H. Wu and Y. Cao, *Nature Photonics,* 2012, **6**, 591-595.

8 R. F. Service, *Science,* 2011, **332**, 293.

9 M. C. Scharber, D. M€uhlbacher, M. Koppe, P. Denk, C. Waldauf, A. J. Heeger and C. J. Brabec, *Adv. Mater,.* 2006, **18**, 789-794.

10 M. A. Green, K. Emery, Y. Hishikawa, W. Warta and E. D. Dunlop, *Prog. Photovolt: Res. Appl.,* 2013, **21**, 1-11.

11 C. R. McNeill and N. C. Greenham, *Adv. Mater.,* 2009, **21**, 3840-3850.

12 J. E. Slota, X. M. He and W. T. S. Huck*, Nano Today,* 2010, **5***,* 231-242.

13 W. Chen, M. P. Nikiforov and S. B. Darling *Energy Environ. Sci.*, 2012, **5**, 8045-8074.

14 F. Padinger, R. S. Rittberger and N. S. Sariciftci, *Adv. Funct. Mater.,* 2003, **13**, 85-88.

15 C. R. McNeill, A. Abrusci, J. Zaumseil, R. Wilson, M. J. McKiernan, J. H. Burroughes, J. J. M. Halls, N. C. Greenham and R. H. Friend, *Appl. Phys. Lett.,* 2007, **90**, 193506.

16 C. R. McNeill, J. J. M. Halls, R. Wilson, G. L. Whiting, S. Berkebile, M. G. Ramsey, R. H. Friend and N. C. Greenham, *Adv. Funct. Mater.,* 2008, **18**, 2309-2321.

17 Y. Zhao, Z. Y. Xie, Y. Qu, Y. H. Geng and L. X. Wang, *Appl. Phys. Lett.,* 2007, **90,** 43504.

18 G. Li, V. Shrotriya, J. Huang, Y. Yao, T. Moriarty, K. Emery and Y. Yang, *Nat. Mater.,* 2005, **4**, 864-868.

19 J. H. Park, J. S. Kim, J. H. Lee, W. H. Lee and K. Cho, *J. Phys. Chem. C,* 2009, **113***,* 17579-17584.

20 J. Peet, J. Y. Kim, N. E. Coates, W. L. Ma, D. Moses, A. J. Heeger and G. C. Bazan, *Nat. Mater.,* 2007, **6***,* 497-500.

21 H.-Y. Chen, H. Yang, G. Yang, S. Sista, R. Zadoyan, G. Li and Y. Yang, *J. Phys. Chem. C,* 2009, **113**, 7946-7963.

22 A. J. Moulé and, K. Meerholz, *Adv. Mater.,* 2008, **20,** 240-245.

23. H.-C. Liao, C.-C. Ho, C.-Y. Chang, M.-H. Jao, S. B. Darling and W.-F. Su. *Materials Today* 2013, **16**, 326-336.

24 J. Peet, C. Soci, R. C. Coffin, T. Q. Nguyen, A. Mikhailovsky, D. Moses and G. C. Bazan, *App. Phys. Lett,,* 2006, **89**, 252105.

25 J. Peet, M. L. Senatore, A. J. Heeger and G. C. Bazan, *Adv. Mater.,* 2009, **21**, 1521-1529.

26 J. K. Lee, W. L. Ma, C. J. Brabec, J. Yuen, J. S. Moon, J. Y. Kim, K. Lee, G. C. Bazan and A. J. Heeger, *J. Am. Chem. Soc.,* 2008, **130**, 3619-3623.

27 M.-S. Su, C.-Y. Kuo, M.-C. Yuan, U.-S. Jeng, C.-J. Su and K.-H. Wei, *Adv. Mater.,*

2011, **23**, 3315-3319.

28 J.-S. Wu, C.-T. Lin, C.-L. Wang, Y.-J. Cheng and C.-S. Hsu, *Chem. Mater.,* 2012, **24,** 2391-2399.

29 J. S. Moon, C. J. Takacs, S. Cho, R. C. Coffin, H. Kim, G. C. Bazan and A. J. Heeger, *Nano Lett.,* 2010, **10**, 40054008.

30 K. S. Nalwa, J. A. Carr, R. C. Mahadevapuram, H. K. Kodali, S. Bose, Y. Chen, J. W. Petrich, B. Ganapathysubramanianc and S. Chaudhary, *Energy Environ. Sci.,* 2012, **5**, 7042-7049.

31 B. Paci, A. Generosi, V. R. Albertini, G. D. Spyropoulos, E. Stratakis and E. Kymakis, *Nanoscale,* 2012, **4**, 7452-7459.

32 S. Jeong, Y. Kwon, B.-D. Choi, H. Ade and Y. S. Han, *Appl. Phys. Lett.,* 2010, **96**, 183305.

33 X. Liu, S. Huettner, Z. Rong, M. Sommer and R. H. Friend, *Adv. Mater.,* 2012, **24**, 669-674.

34 J. U. Lee, J. W. Jung, T. Emrick, T. P. Russell and W. H. Jo, *J. Mater. Chem.,* 2010, **20**, 3287-3294.

35 K. Sivula, Z. T. Ball, N. Watanabe and J. M. J. Frechet, *Adv. Mater.*, 2006, **18**, 206-210.

36 C. Yang, J. K. Lee, A. J. Heeger and F. Wudl, *J. Mater. Chem.,* 2009, **19**, 5416-5423.

37 J. U. Lee, A. Cirpan, T. Emrick, T. P. Russell and W. H. Jo, *Nanotechnology,* 2010, **21**, 105201.

38 R. Lecover, N. Williams, N. Markovic, D. H. Reich, D. Q. Naiman and H. E. Katz, *ACS Nano,* 2012, **6**, 2865–2870.

39 J. K. Lee, W. L. Ma, C. J. Brabec, J. Yuen, J. S. Moon, J. Y. Kim, K. Lee, G. C. Bazan and A. J. Heeger, *J. Am. Chem. Soc.,* 2008, **130**, 3619-3623.

40 L. Bakueva, D. Matheson, S Musikhin and E. H. Sargent, *Synth. Met.,* 2002, **126**, 207–211.

41 G. Li, Y. Yao, H. Yang, V. Shrotriya, G. Yang and Y. Yang, *Adv. Funct. Mater.,* 2007, **17**, 1636-1644.

42 F. C. Spano, *J. Chem. Phys.,* 2005, **122**, 234701.

43 U. Zhokhavets, T. Erb, G. Gobsch, M. Al-Ibrahim and O. Ambacher, *Chem. Phys. Lett.,* 2006, **418**, 347-350.

44 R. Osterbacka, C. P. An, X. M. Jiang and Z. V. Vardeny, *Science,* 2000*,* **287**, 839-842.

45 J. Clark, J. F. Chang, F. Spano, R. H. Friend and C. Silva, *Appl. Phys. Lett.,* 2009, **94***,* 163306.

46 Y. Kim, S. A. Choulis, J. Nelson, D. D. C. Bradley, S. Cook and J. R. Durrant, *J. Mater. Sci.,* 2005, **40**, 1371-1379.

47 J. Gao, F. Hide and H. Wang, *Synth. Met.,* 1997, **84**, 979-980.

48 C. Lee, G. Yu, D. Moses, K. Pakbaz, C. Zhang, N. Sariciftci, A. Heeger and F. Wudl, *Phys. Rev. B,* 1993, **48**, 15425-15433.

49 L. Smilowitz, N. S. Sariciftci, R. Wu, C. Gettinger, A. J. Heeger and F. Wudl, *Phys. Rev. B,* 1993, **47**, 1383-1391.

50 C.-W. Liang, W.-F., Su and L. Wang, *Appl. Phys. Lett.,* 2009, **95**, 133303.

51 G. Li, V. Shrotriya, J. Huang, Y. Yao, T. Moriarty, K. Emery and Y. Yang, *Nature Mater.,* 2005, **4**, 864–868.

52 W. L. Ma, C. Y. Yang, X. Gong, K. Lee and A. J.Heeger, *Adv. Funct. Mater.,* 2005, **15**, 1617–1622.

53 X. N. Yang, J. Loos, S. C. Veenstra, W. J. H. Verhees, M. M. Wienk, J. M. Kroon, M. A. J. Michels and R. A. J. Janssen, *Nano Lett.,* 2005, **5**, 579-583.

54 M. Campoy-Quiles, T. Ferenczi, T. Agostinelli, P. G. Etchegoin, Y. Kim, T. D.

Anthopoulos, P. N. Stavrinou, D. D. C. Bradley and J. Nelson, *Nat. Mater.,* 2008, **7**, 158-164.

55 J. Peet, A. J. Heeger and G. C. Bazan, *Acc. Chem. Res.,* 2009, 42, 1700-1708.

56 D. A. Chen, A. Nakahara, D. G. Wei, D. Nordlund and T. P. Russell, *Nano Lett.,* 2011, **11**, 561-567.

57 N. D. Treat, M. A. Brady, G. Smith, M. F. Toney, E. J. Kramer, C. J. Hawker and M. L. Chabinyc, *Adv. Energy Mater.,* 2011, **1,** 82-89.

58 A. J. Moulé and K. Meerholz, *Adv. Mater.,* 2008, **20,** 240–245.

59 V. Shrotriya, Y. Yao, G. Li and Y. Yang, *Appl. Phys. Lett.,* 2006, **89**, 063505.

60 Y.-H. Chen, P.-T. Huang, K.-C. Lin, Y.-J. Huang and C.-T. Chen, *Org. Electron.,* 2012, **13**, 283-289.

61 G. Zhao, Y. He and Y. Li, *Adv. Mater.,* 2010, **22**, 4355–4358.

Figure captions

Figure 1: *I-V* curves of the devices based on P3HT/$PC_{61}BM$ blended film with or without additive fabricated with or without thermal annealing.

Figure 2: (a) Uv/Vis absorption and PL spectra of P3HT/$PC_{61}BM$ films with or without additive fabricated with or without thermal annealing. (b) EQE curves for the devices based on P3HT/$PC_{61}BM$ active films with or without additive fabricated with or without thermal annealing.

Figure 3: AFM topographic (left) and Phase (right) images of P3HT/$PC_{61}BM$ blended films with or without additive fabricated with or without thermal annealing.

Figure 4: Depth profile ESCA analysis of non-thermal P3HT/$PC_{61}BM$ films with and without additive.

Figure 5: ^{1}H-NMR spectra of 2,3-pyridinediol and 2,3-pyridinediol mixed with $PC_{61}BM$. (the peaks between 6~ 8 ppm)

Figure 6: The possible interactions between 2,3-pyridinediol and P3HT (or $PC_{61}BM$).

Table 1: Photovoltaic parameters and hole-only mobility of BHJ-PSC based on P3HT/$PC_{61}BM$ with or without additive fabricated in the different conditions.

Additive	Thermal	Film thickness	*Jsc* (mA/cm^2) (avg.)	*Voc* (V) (avg.)	FF (avg.)	PCE (%) (avg.)/(# cell)	Mobility (cm^2/Vs)
none	**without**	**347 nm**	**5.48±0.93 (4.75)**	**0.61±0.02 (0.60)**	**0.39±0.13 (0.52)**	**1.29±0.25 (1.53)/(8)**	**3.9×10^{-4}**
with	**without**	**350 nm**	**10.6±0.18 (10.71)**	**0.61±0 (0.61)**	**0.66±0.01 (0.67)**	**4.34±0.08 (4.44)/(8)**	**5.8×10^{-3}**
with	**with**	**347 nm**	**9.62±0.10 (9.71)**	**0.62±0 (0.62)**	**0.67±0.11 (0.68)**	**4.00±0.07 (4.07)/(8)**	**3.6×10^{-3}**
none	**with**	**342 nm**	**8.57±0.10 (8.67)**	**0.63±0 (0.63)**	**0.64±0.01 (0.63)**	**3.51±0.06 (3.55)/(8)**	**3.8×10^{-3}**

P3HT:$PC_{61}BM$= 1:1 (in weight). Thermal annealing: 150 ^{o}C, 30 min.

Additive: 2,3-pyridinediol, 20 mg in 1 mL dichlorobenzene.

The photovoltaic performance data were obtained from 8 devices.

Table 2: Photovoltaic parameters of BHJ-PSC based on P3HT/$PC_{61}BM$ with additive at various thicknesses (controlled with spin rate).

Film thickness (nm)[a]	*Jsc* (mA/cm^2) (avg.)	*Voc* (V) (avg.)	FF (avg.)	PCE *(%)* (avg.)/(# cell)
282	9.95±0.19 (9.83)	0.60±0 (0.60)	0.61±0.01 (0.62)	3.61±0.05 (3.65)/(6)
297	9.45±0.25 (9.68)	0.61±0.03 (0.62)	0.61±0.02 (0.61)	3.80±0.08 (3.85)/(6)
320	10.03±0.2 (10.11)	0.60±0 (0.60)	0.62±0.02 (0.63)	3.85±0.08 (3.90)/(6)
350	10.64±0.12 (10.71)	0.61±0 (0.61)	0.66±0.01 (0.67)	4.34±0.08 (4.44)/(8)
390	10.42±0.12 (10.61)	0.60±0 (0.60)	0.60±0.08 (0.61)	3.84±0.05 (3.96)/(6)

a : The thickness value includes 30 nm of PEDOT:PSS film.

P3HT:$PC_{61}BM$= 1:1 (in weight) without thermal treatment.

Additive: 2,3-pyridinediol, 20 mg in 1 mL dichlorobenzene

The photovoltaic performance data were obtained from 6 ~ 8 devices.

Table 3: The effect of 2,3-pyridinediol additive on the photovoltaic parameters of the devices based on P3HT/ICBA and PTB7/$PC_{71}BM$ active films without thermal annealing.

Active layer	**Additive**	***Jsc*** **(mA/cm^2)**	***Voc*** **(V)**	**FF**	**PCE (%)**
P3HT/ICBA	none	6.88	0.81	0.60	3.35
P3HT/ICBA	with	11.78	0.82	0.61	5.93
PTB7:$PC_{71}BM$	none	15.15	0.76	0.47	5.46
PTB7:$PC_{71}BM$	with	18.35	0.77	0.53	7.54

The concentrations of pyridinediol are 0.5wt% and 3 wt% in DCB for P3HT/ICBA and PBT7/$PC_{71}BM$ system, respectively.

Figure 1

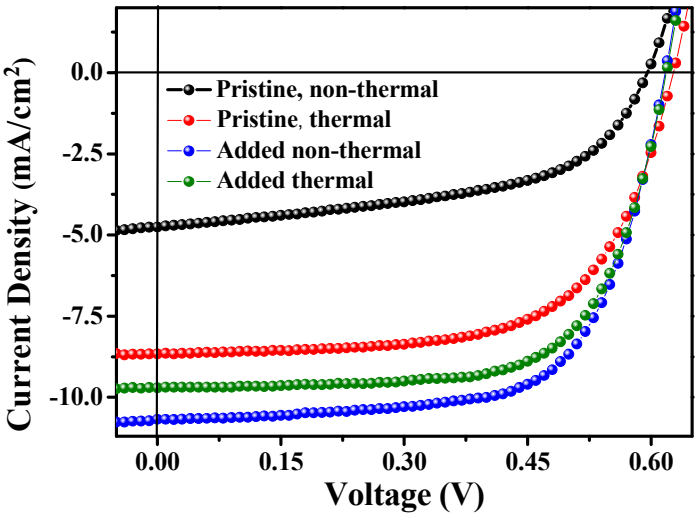

Figure 2

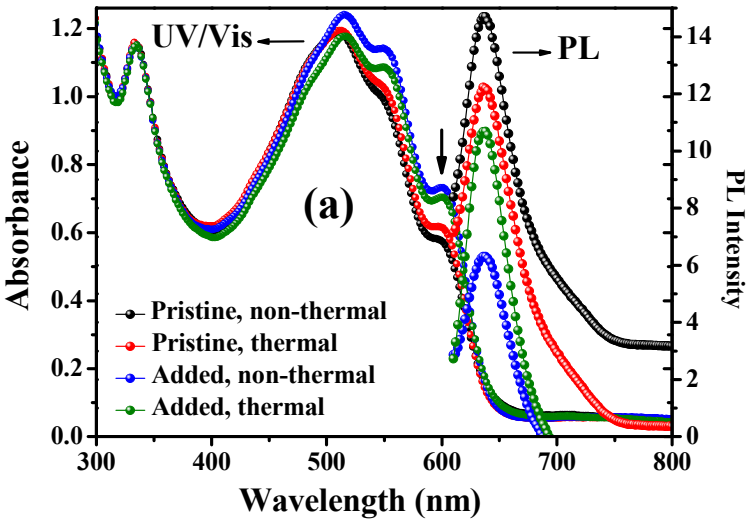

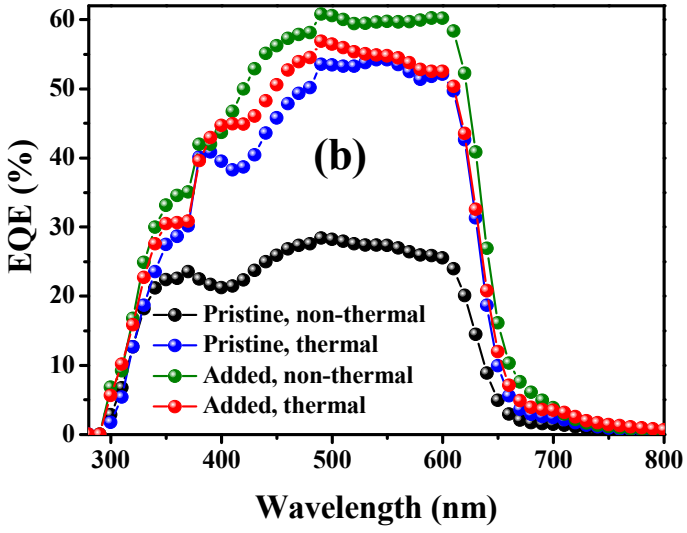

Figure 3

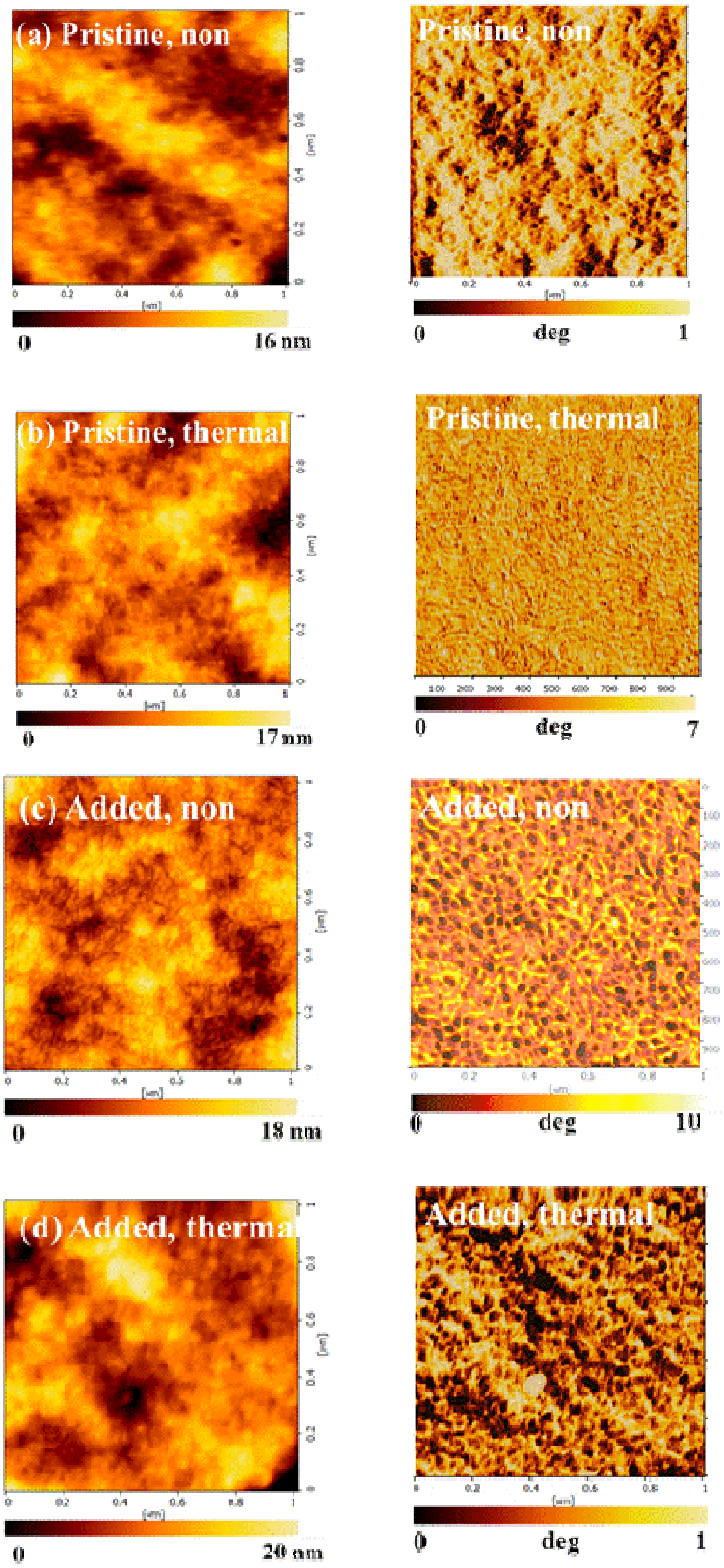

Figure 4

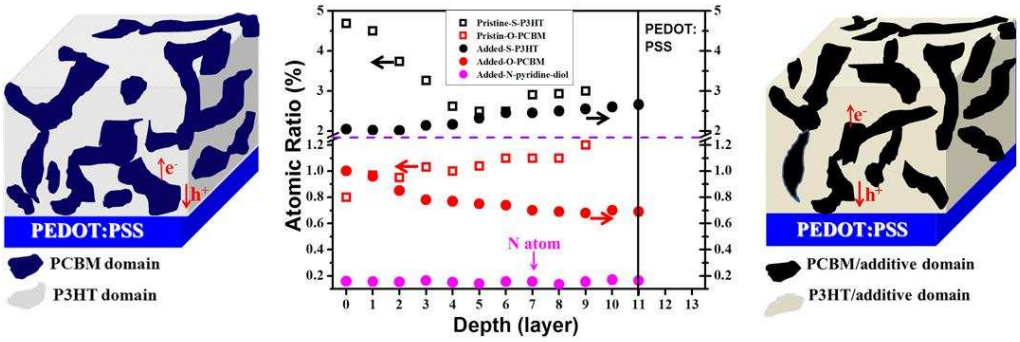

Figure 5

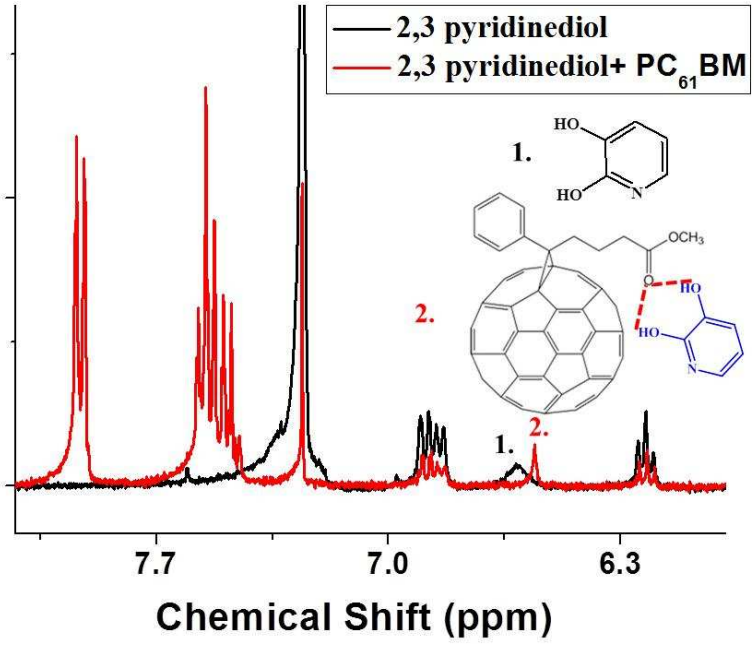

Figure 6

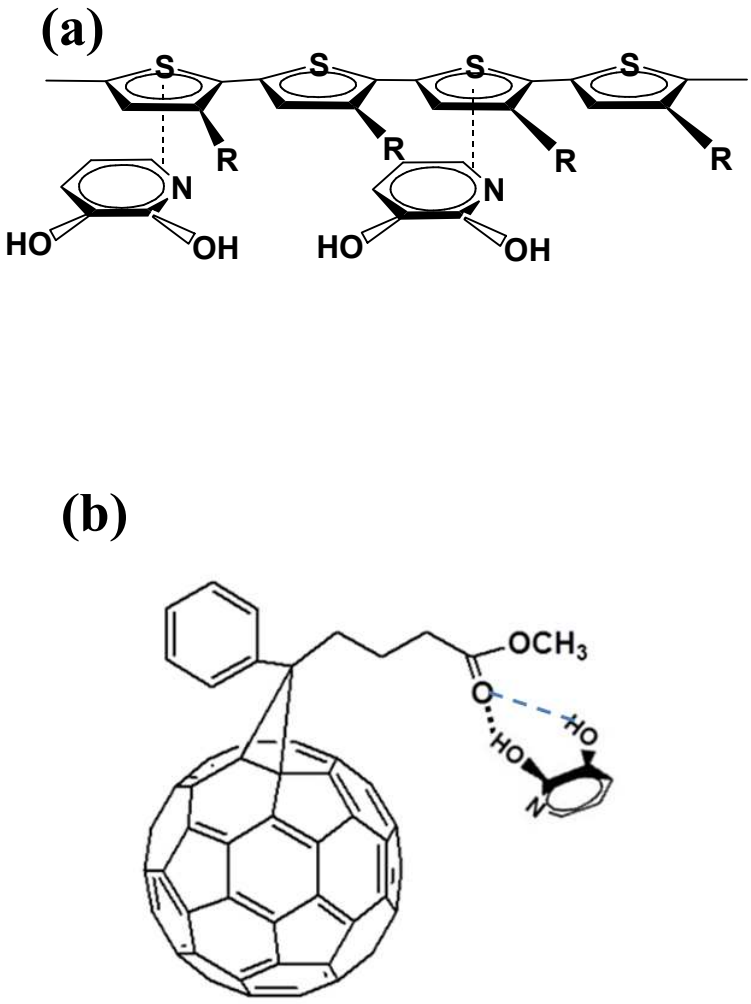

Graphical abstract